Chapter 8 Flow in Conduits

Entrance and developed flows

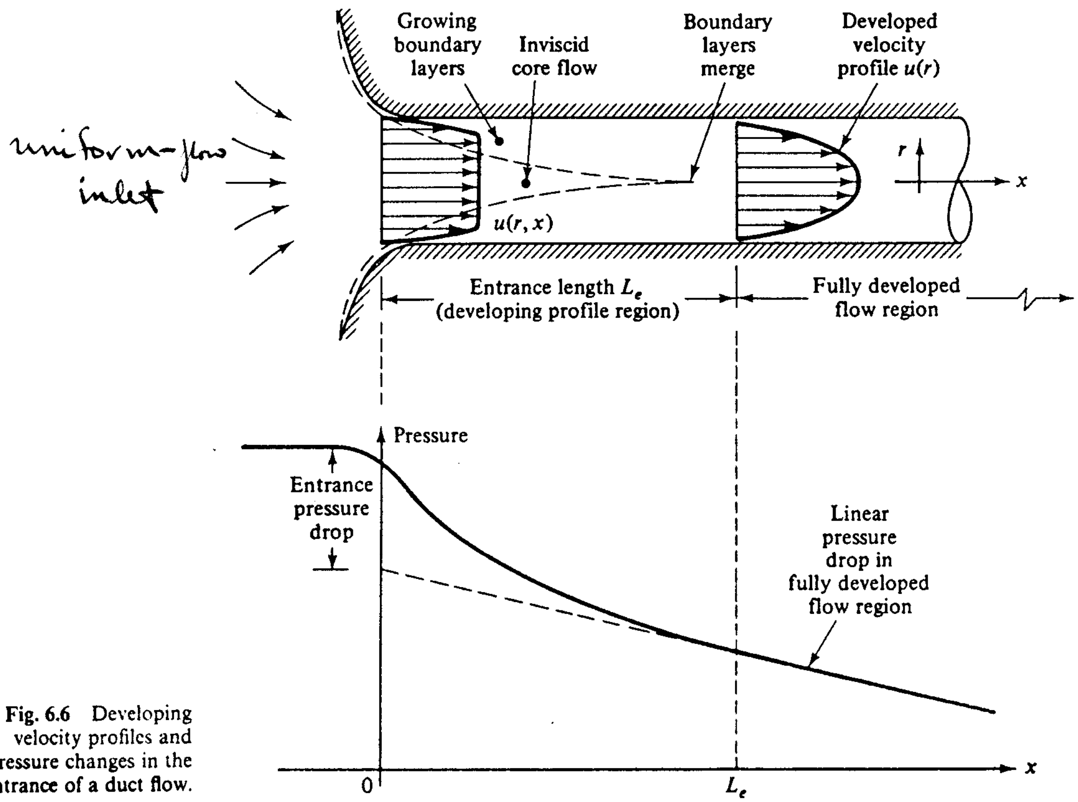

Fig. 6.6 Developing velocity profiles and pressure changes in the entrance of a duct flow.

$$Le = f(D, V, \rho, \mu)$$

Π_i theorem $\Rightarrow$ $Le/D = f(Re)$

Laminar flow: $Re_{crit} \sim 2000$, i.e., for $Re < Re_{crit}$ laminar
$Re > Re_{crit}$ turbulent

$Le/D = .06Re$ from experiments

$Le_{max} = .06Re_{crit}D \sim 138D$

maximum Le for laminar flow

Turbulent flow:

$$\frac{Le}{D} \sim 4.4\,Re^{1/6}$$

from experiment

Re	Le/D
4000	18
10^4	20
10^5	30
10^6	44
10^7	65
10^8	95

i.e., relatively shorter than for laminar flow

Laminar vs. Turbulent Flow

Hagen 1839 noted difference in $\Delta p = \Delta p(V)$ but could not explain two regimes

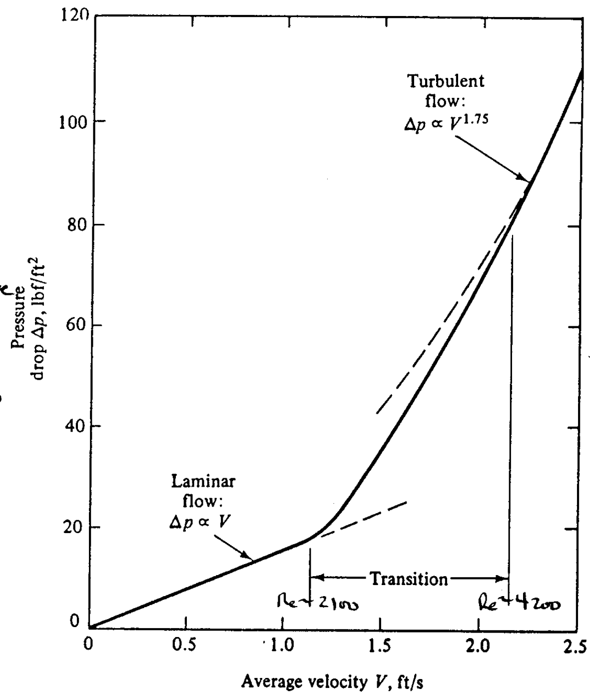

Fig. 6.4 Experimental evidence of transition for water flow in a $\frac{1}{2}$-in smooth pipe 10 ft long.

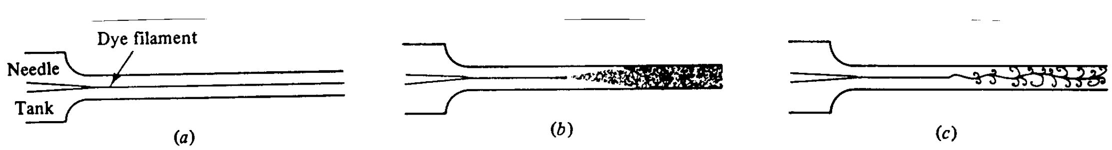

laminar turbulent spark photo

Reynolds 1883 showed difference depends on $Re = \dfrac{VD}{\nu}$

Shear-Stress Distribution Across a Pipe Section

Continuity: $Q_1 = Q_2 = \text{constant}$

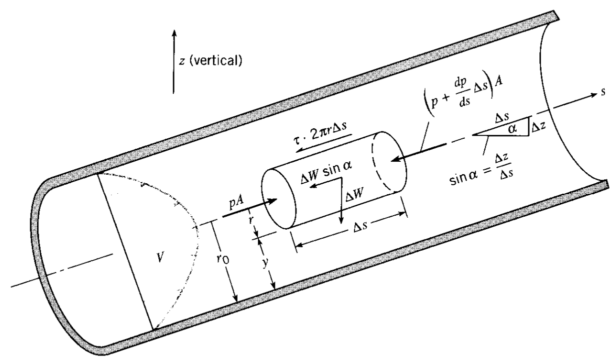

FIGURE 10.1
Variation of shear stress in a pipe.

i.e., $V_1 = V_2$ since $A_1 = A_2$

Momentum: $\sum F_s = \sum \rho u(\underline{V} \cdot \underline{A})$

$$= \rho V_1(-V_1 A_1) - \rho V_2(V_2 A_2)$$

$$= \rho Q(V_2 - V_1) = 0$$

$$pA - \left(p + \frac{dp}{ds} ds\right)A - \Delta W \sin\alpha - \tau(2\pi r)ds = 0$$

$\Delta W = \gamma A ds$ $\qquad$ $\sin\alpha = \dfrac{dz}{ds}$

$$-\frac{dp}{ds} dsA - \gamma A ds \frac{dz}{ds} - \tau(2\pi r)ds = 0$$

$\div$ Ads $\qquad$ $\tau = \dfrac{r}{2}\left[-\dfrac{d}{ds}(p + \gamma z)\right]$

τ varies linearly from 0.0 at r = 0 (centerline) to τ_{max} (= τ_w) at r = R (wall). Valid for laminar and turbulent flow.

Laminar Flow in Pipes

$$\tau = \mu \frac{dV}{dy} = -\mu \frac{dV}{dr} = \frac{r}{2}\left[-\frac{d}{ds}(p+\gamma z)\right]$$

$$y = \text{wall coordinate} = r_o - r \Rightarrow \frac{dV}{dr} = \frac{dV}{dy}\frac{dy}{dr} = -\frac{dV}{dy}$$

$$\frac{dV}{dr} = -\frac{r}{2\mu}\left[-\frac{d}{ds}(p+\gamma z)\right]$$

$$V = -\frac{r^2}{4\mu}\left[-\frac{d}{ds}(p+\gamma z)\right] + C$$

$$\underbrace{V(r_o) = 0}_{\text{no slip condition}} \Rightarrow C = \frac{r_o^2}{4\mu}\left[-\frac{d}{ds}(p+\gamma z)\right]$$

$$V(r) = \frac{r_o^2 - r^2}{4\mu}\left[-\frac{d}{ds}(p+\gamma z)\right]$$

Exact solution to Navier-Stokes equations for laminar flow in circular pipe

$$Q = \int \underline{V} \cdot d\underline{A}$$

$$= \int_0^{r_o} V(r) \underbrace{2\pi r dr}$$

$$V_{max} = \frac{r_o^2}{4\mu}\left[-\frac{d}{ds}(p+\gamma z)\right]$$

$$dA = r dr d\theta = r dr(2\pi)$$

$$Q = \frac{\pi r_o^4}{8\mu}\left[-\frac{d}{ds}(p+\gamma z)\right]$$

$$\overline{V} = \frac{Q}{A} = \frac{r_o^2}{8\mu}\left[-\frac{d}{ds}(p+\gamma z)\right]$$

$$\overline{V} = \frac{V_{max}}{2}$$

FIGURE 10.2
Distribution of shear stress and velocity for laminar flow in a pipe.

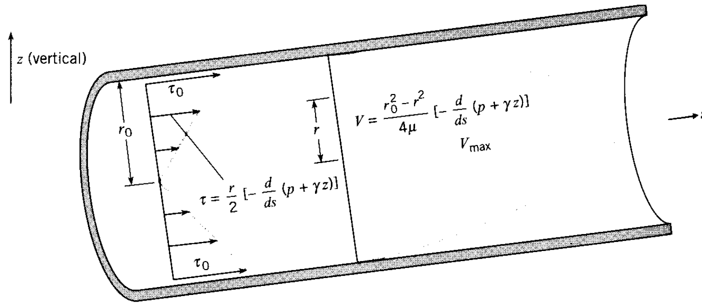

energy equation:

$$\frac{p_1}{\gamma} + \frac{V_1^2}{2g} + z_1 = \frac{p_2}{\gamma} + \frac{V_2^2}{2g} + z_2 + h_L$$

$$\Delta h = \left(\frac{p_2}{\gamma} + z_2\right) - \left(\frac{p_1}{\gamma} + z_1\right)$$

$$h_L = \frac{p_1 - p_2}{\gamma} + (z_1 - z_2) = -\Delta h$$

$$h_L = \frac{L}{\gamma}\left[-\frac{d}{ds}(p + \gamma z)\right]$$

L = length of pipe = ds

$$h_L = L\left[-\frac{d}{ds}\left(\frac{p}{\gamma} + z\right)\right]$$

$$= L\left(-\frac{dh}{ds}\right)$$

$$= \frac{L}{\gamma}\left[\frac{8\mu\overline{V}}{r_o^2}\right] = -\Delta h \alpha \overline{V}$$

or $\quad h_f = h_L = \dfrac{32\mu L\overline{V}}{\gamma D^2}$ $\qquad h_f$ = head loss due to friction

exact solution

$$\underbrace{\text{friction factor } f = \frac{8\tau_w}{\rho\overline{V}^2}}_{\text{friction coefficient for pipe flow}} \qquad \underbrace{C_f = \frac{\tau_w}{\frac{1}{2}\rho V^2}}_{\text{boundary layer flow}}$$

$$\tau_w = \frac{r_o}{2}\left[-\frac{d}{ds}(p+\gamma z)\right]$$

$$= \frac{r_o}{2}\left[\frac{8\mu\overline{V}}{r_o^2}\right]$$

$$\tau_w = \frac{4\mu\overline{V}}{r_o}$$

$$f = \frac{32\mu}{\rho r_o \overline{V}} = \frac{64\mu}{\rho\overline{V}D} = \frac{64}{Re} \qquad \text{exact solution}$$

$$Re = \frac{\overline{V}D}{\nu} \qquad \nu = \frac{\mu}{\rho}$$

Criterion for Laminar or Turbulent Flow in a Pipe

$Re_{crit} \sim 2000$ flow becomes unstable
$Re_{trans} \sim 3000$ flow becomes turbulent
$Re = \overline{V}D/\nu$

Turbulent Flow in Pipes

Continuity and momentum:

$$\tau(r = r_o) = \tau_o = \frac{r_o}{2}\left[-\frac{d}{ds}(p + \gamma z)\right]$$

Energy: $h_f = \dfrac{L}{\gamma}\left[-\dfrac{d}{ds}(p + \gamma z)\right]$

Combining: $h_f = \dfrac{L}{\gamma} \cdot \dfrac{2\tau_o}{r_o}$ define $f = \dfrac{\tau_o}{\frac{1}{8}\rho\overline{V}^2}$ = friction factor

$$h_f = \frac{L}{\rho g} \cdot \frac{2}{r_o} \cdot \frac{1}{8}\rho\overline{V}^2 f$$

$$h_f = f \cdot \frac{L}{D} \cdot \frac{\overline{V}^2}{2g}$$ Darcy – Weisbach Equation

f = f(Re, k/D) = still must be determined!

$Re = \dfrac{\overline{V}D}{\nu}$ k = roughness

Description of Turbulent Flow

Most flows in engineering are turbulent: flows over vehicles (airplane, ship, train, car), internal flows (heating and ventilation, turbo-machinery), and geophysical flows (atmosphere, ocean).

$\underline{v}$ ($\underline{x}$, t) and p($\underline{x}$, t) are random functions of space and time, but statistically stationary flaws such as steady and forced or dominant frequency unsteady flows display coherent features and are amendable to statistical analysis, i.e. time and place (conditional) averaging. RMS and other low-order statistical quantification can be modeled and used in conjunction with averaged equations for solving practical engineering problems.

Turbulent motions range in size from the width in the flow δ to much smaller scales, which come progressively smaller as the Re = $U\delta/\upsilon$ increases.

Fig. 1.1. A photograph of the turbulent plume from the ground test of a Titan IV rocket motor. The nozzle's exit diameter is 3 m, the estimated plume height is 1,500 m, and the estimated Reynolds number is 200×10^6. For more details see Mungal and Hollingsworth (1989). With permission of San Jose Mercury & News.

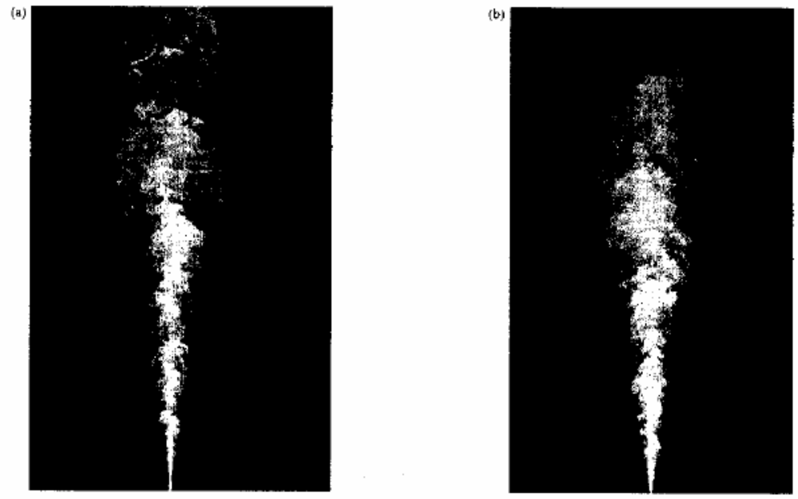

Fig. 1.2. Planar images of concentration in a turbulent jet: (a) Re = 5,000 and (b) Re = 20,000. From Dahm and Dimotakis (1990).

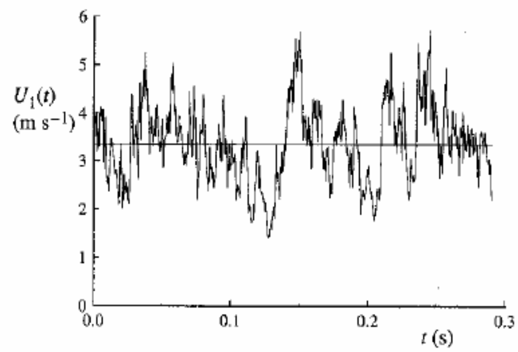

Fig. 1.3. The time history of the axial component of velocity $U_1(t)$ on the centerline of a turbulent jet. From the experiment of Tong and Warhaft (1995).

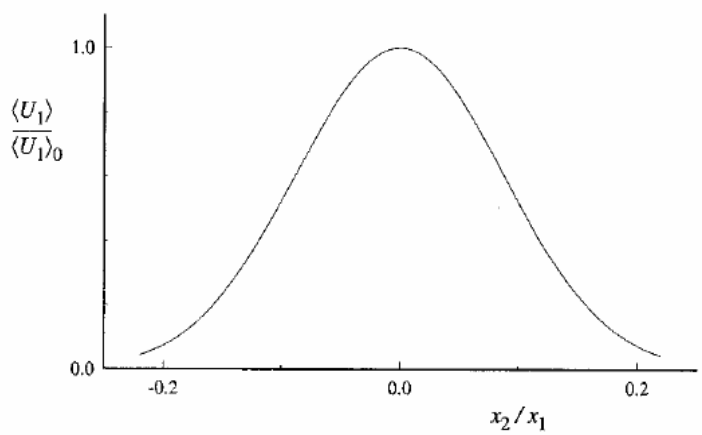

Fig. 1.4. The mean axial velocity profile in a turbulent jet. The mean velocity $\langle U_1 \rangle$ is normalized by its value on the centerline, $\langle U_1 \rangle_0$; and the cross-stream (radial) coordinate x_2 is normalized by the distance from the nozzle x_1. The Reynolds number is 95,500. Adapted from Hussein, Capp, and George (1994).

Physical description:

(1) Randomness and fluctuations:

Turbulence is irregular, chaotic, and unpredictable. However, structurally stationary flows, such as steady flows, can be analyzed using Reynolds decomposition.

$$u = \overline{u} + u' \qquad \overline{u} = \frac{1}{T}\int_{t_0}^{t_0+T} u\, dT \qquad \overline{u'} = 0 \qquad \overline{u'^2} = \frac{1}{T}\int_{t_0}^{t_0+T} u'^2\, dT$$

etc.

$\overline{u}$ = mean motion
u' = superimposed random fluctuation
$\overline{u'^2}$= Reynolds stresses; RMS = $\sqrt{\overline{u'^2}}$

Triple decomposition is used for forced or dominant frequency flows

$$u = \overline{u} + u'' + u'$$

Where u'' = organized component

(2) Nonlinearity

Reynolds stresses and 3D vortex stretching are direct results of nonlinear nature of turbulence. In fact, Reynolds stresses arise from nonlinear convection term after substitution of Reynolds decomposition into NS equations and time averaging.

(3) Diffusion

Large scale mixing of fluid particles greatly enhances diffusion of momentum (and heat), i.e.,

Reynolds Stresses: $$-\rho\overline{u'_i u'_j} >> \overbrace{\tau_{ij} = \mu\varepsilon_{ij}}^{viscous\ stress}$$

Isotropic eddy viscosity: $$-\overline{u'_i u'_j} >> \upsilon_t \varepsilon_{ij} - \frac{2}{3}\delta_{ij}k$$

(4) Vorticity/eddies/energy cascade

Turbulence is characterized by flow visualization as eddies, which vary in size from the largest L_δ (width of flow) to the smallest. The largest eddies have velocity scale U and time scale L_δ/U. The orders of magnitude of the smallest eddies (Kolmogorov scale or inner scale) are:

L_K = Kolmogorov micro-scale = $\left[\dfrac{\upsilon^3 \delta}{U^3}\right]^{\frac{1}{4}}$

L_K = O(mm) >> $L_{\text{mean free path}} = 6 \times 10^{-8}$ m

Velocity scale = $(\nu\varepsilon)^{1/4}$= O(10^{-2}m/s)

Time scale = $(\nu/\varepsilon)^{1/2}$= O(10^{-2}s)

Largest eddies contain most of energy, which break up into successively smaller eddies with energy transfer to yet smaller eddies until L_K is reached and energy is dissipated by molecular viscosity (i.e. viscous diffusion).

Richardson (1922):

L_δ Big whorls have little whorls
Which feed on their velocity;
And little whorls have lesser whorls,
L_K And so on to viscosity (in the molecular sense).

(5) Dissipation

$$\ell_0 = L_\delta$$

$$u_0 = \sqrt{k} \qquad k = \overline{u'^2} + \overline{v'^2} + \overline{w'^2}$$

$$= 0(U)$$

$$\mathrm{Re}_\delta = u_0 \ell_0 / \upsilon = big$$

$\rightarrow$ Energy comes from largest scales and fed by mean motion

ε = rate of dissipation = energy/time

$$= u_0^2 / \tau_o \qquad \tau_o = \ell_0 / u_0$$

$$= u_0^3 / l_0 \quad \text{independent } \upsilon \qquad L_K = \left[\frac{\upsilon^3}{\varepsilon}\right]^{\frac{1}{4}}$$

$\rightarrow$ Dissipation occurs at smallest scales

The mathematical complexity of turbulence entirely precludes any exact analysis. A statistical theory is well developed; however, it is both beyond the scope of this course and not generally useful as a predictive tool. Since the time of Reynolds (1883) turbulent flows have been analyzed by considering the mean (time averaged) motion and the influence of turbulence on it; that is, we separate the velocity and pressure fields into mean and fluctuating components.

It is generally assumed (following Reynolds) that the motion can be separated into a mean ($\overline{u}$, $\overline{v}$, $\overline{w}$, p) and superimposed turbulent fluctuating (u', v', w', p') components, where the mean values of the latter are 0.

$$u = \overline{u} + u' \qquad p = \overline{p} + p'$$

$$v = \overline{v} + v' \qquad \text{and for compressible flow}$$

$$w = \overline{w} + w' \qquad \rho = \overline{\rho} + \rho' \text{ and } T = \overline{T} + T'$$

where (for example)

$$\overline{u} = \frac{1}{t_1}\int_{t_0}^{t_0+t_1} u\,dt$$

and t_1 sufficiently large that the average is independent of time

Thus by definition $\overline{u'} = 0$, etc. Also, note the following rules which apply to two dependent variables f and g

$$\overline{\overline{f}} = \overline{f} \qquad \overline{f+g} = \overline{f} + \overline{g}$$

$$\overline{\overline{f}\cdot g} = \overline{f}\cdot\overline{g}$$

$$\overline{\frac{\partial f}{\partial s}} = \frac{\partial \overline{f}}{\partial s} \qquad \overline{\int f ds} = \int \overline{f} ds$$

$f = (u, v, w, p)$
$s = (x, y, z, t)$

The most important influence of turbulence on the mean motion is an increase in the fluid stress due to what are called the apparent stresses. Also known as Reynolds stresses:

$$\tau'_{ij} = -\rho \overline{u'_i u'_j}$$

$$= \begin{bmatrix} -\rho\overline{u'^2} & -\rho\overline{u'v'} & -\rho\overline{u'w'} \\ -\rho\overline{u'v'} & -\rho\overline{v'^2} & -\rho\overline{v'w'} \\ -\rho\overline{u'w'} & -\rho\overline{v'w'} & -\rho\overline{w'^2} \end{bmatrix}$$

Symmetric 2^{nd} order tensor

The mean-flow equations for turbulent flow are derived by substituting $\underline{V} = \underline{\overline{V}} + \underline{V'}$ into the Navier-Stokes equations and averaging. The resulting equations, which are called the Reynolds-averaged Navier-Stokes (RANS) equations are:

Continuity $\quad \nabla \cdot \underline{V} = 0 \quad$ i.e. $\nabla \cdot \underline{\overline{V}} = 0$ and $\nabla \cdot \underline{V'} = 0$

Momentum $\quad \rho \dfrac{D\overline{V}}{Dt} + \rho \dfrac{\partial}{\partial x_j}\left(\overline{u'_i u'_j}\right) = -\rho g\hat{k} - \nabla \overline{p} + \mu \nabla^2 \underline{\overline{V}}$

or $\quad \rho \dfrac{D\overline{V}}{Dt} = -\rho g\hat{k} - \nabla \overline{p} + \nabla \cdot \tau_{ij}$

$$\tau_{ij} = \mu\left[\frac{\partial u_i}{\partial x_j} + \frac{\partial u_j}{\partial x_i}\right] \underbrace{-\rho\overline{u'_i u'_j}}_{\tau'_{ij}}$$

$u_1 = u \qquad x_1 = x$
$u_2 = v \qquad x_2 = y$
$u_3 = w \qquad x_3 = z$

Comments:

1) equations are for the mean flow
2) differ from laminar equations by Reynolds stress terms = $\overline{u_i' u_j'}$
3) influence of turbulence is to transport momentum from one point to another in a similar manner as viscosity
4) since $\overline{u_i' u_j'}$ are unknown, the problem is indeterminate: the central problem of turbulent flow analysis is closure!

4 equations and 4 + 6 = 10 unknowns

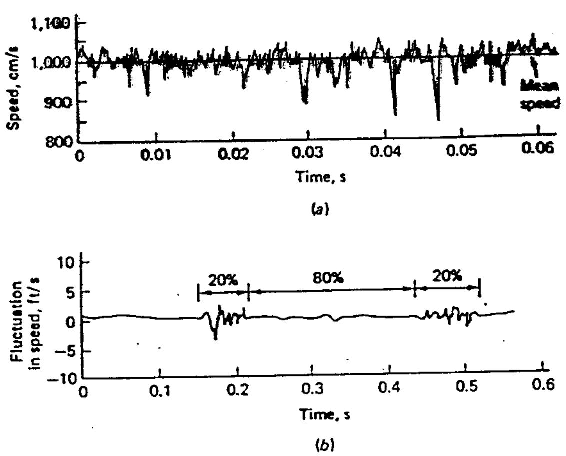

FIGURE 5-35
Hot-wire measurements showing turbulent velocity fluctuations: (*a*) typical trace of a single velocity component in a turbulent flow; (*b*) trace showing intermittent turbulence at the edge of a jet.

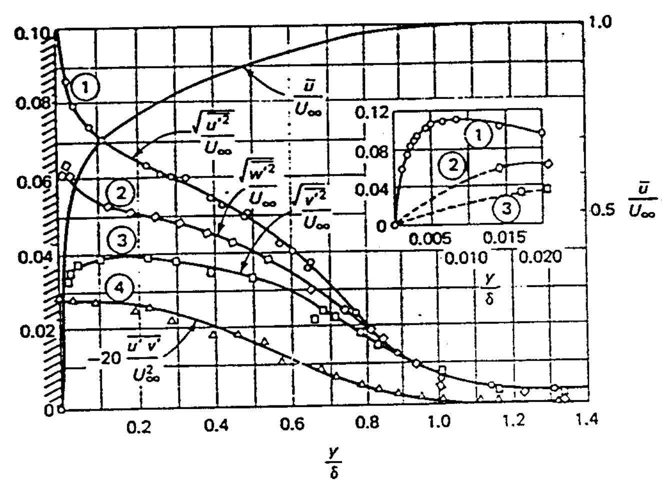

FIGURE 5-36
Flat-plate measurements of the fluctuating velocities u' (streamwise), (normal), and w' (lateral) and the turbulent shear $u'v'$. [*After Klebanoff* (*1955*).]

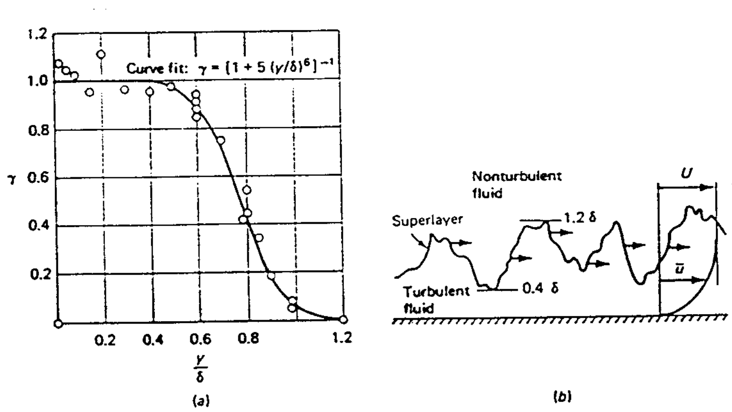

FIGURE 5-37
The phenomenon of intermittency in a turbulent boundary layer: (a) measured intermittency factors [*after Klebanoff (1955)*]; (b) the superlayer interface between turbulent and nonturbulent fluid.

$$\psi = \frac{\overline{u'v'}}{\sqrt{\overline{u'^2}}\cdot\sqrt{\overline{v'^2}}}$$

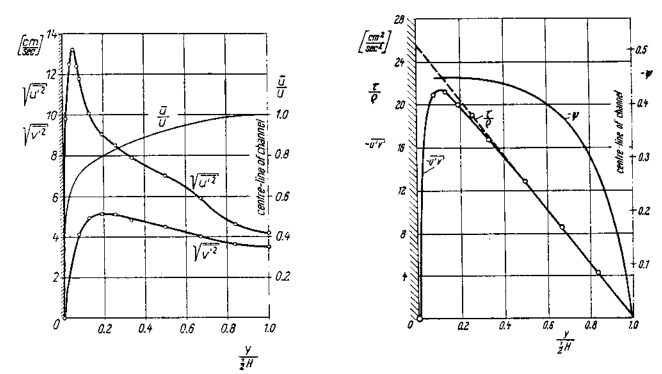

Fig. 18.3. Measurement of fluctuating turbulent components in a wind tunnel, at maximum velocity U = 100 cm/sec after Reichardt [41]
Root-mean-square of longitudinal fluctuation $\sqrt{\overline{u'^2}}$, transverse fluctuation $\sqrt{\overline{v'^2}}$, mean velocity $\bar{u}$

Fig. 18.4. Measurement of fluctuating components in a channel, after Reichardt [41]
The product $\overline{u'v'}$, the shearing stress τ/ϱ, and the correlation coefficient ψ

Turbulence Modeling

Closure of the turbulent RANS equations require the determination of $-\rho\overline{u'v'}$, etc. Historically, two approaches were developed: (a) eddy viscosity theories in which the Reynolds stresses are modeled directly as a function of local geometry and flow conditions; and (b) mean-flow velocity profile correlations which model the mean-flow profile itself. The modern approaches, which are beyond the scope of this class, involve the solution for transport PDE's for the Reynolds stresses which are solved in conjunction with the momentum equations.

(a) eddy-viscosity: theories
(mainly used with differential methods)

$$-\rho\overline{u'v'} = \mu_t \frac{\partial \overline{u}}{\partial y}$$

In analogy with the laminar viscous stress, i.e., $\tau_t \propto$ mean-flow rate of strain

The problem is reduced to modeling μ_t, i.e.,

$$\mu_t = \mu_t(\underline{x}, \text{flow at hand})$$

Various levels of sophistication presently exist in modeling μ_t

$$\mu_t = \underbrace{\rho V_t}_{\text{turbulent velocity scale}} \underbrace{L_t}_{\text{turbulent length scale}}$$

where V_t and L_t are based an large scale turbulent motion

The total stress is

$$\tau_{total} = (\underbrace{\mu}_{\text{molecular viscosity}} + \underbrace{\mu_t}_{\text{eddy viscosity (for high Re flow } \mu_t >> \mu)})\frac{\partial \overline{u}}{\partial y}$$

Mixing-length theory (Prandtl, 1920)

$$-\rho\overline{u'v'} = c\rho\sqrt{\overline{u'^2}}\sqrt{\overline{v'^2}}$$

based on kinetic theory of gases

$$\sqrt{\overline{u'^2}} = \ell_1 \frac{\partial \overline{u}}{\partial y}$$

$$\sqrt{\overline{v'^2}} = \ell_2 \frac{\partial \overline{u}}{\partial y}$$

ℓ_1 and ℓ_2 are mixing lengths which are analogous to molecular mean free path, but much larger

$$\Rightarrow \quad -\rho\overline{u'v'} = \rho\ell^2 \left|\frac{\partial \overline{u}}{\partial y}\right| \frac{\partial \overline{u}}{\partial y}$$

Known as a zero equation model since no additional PDE's are solved, only an algebraic relation

distance across shear layer

$$\ell = \ell(y)$$

= f(boundary layer, jet, wake, etc.)

Although mixing-length theory has provided a very useful tool for engineering analysis, it lacks generality. Therefore, more general methods have been developed.

One and two equation models

$$\mu_t = \frac{C\rho k}{\varepsilon}$$

C = constant

k = turbulent kinetic energy

$= \overline{u'^2 + v'^2 + w'^2}$

ε = turbulent dissipation rate

Governing PDE's are derived for k and ε which contain terms that require additional modeling. Although more general then the zero-equation models, the k-ε model also has definite limitation; therefore, recent work involves the solution of PDE's for the Reynolds stresses themselves. Difficulty is that these contain triple correlations that are very difficult to model.

(b) mean-flow velocity profile correlations
(mainly used with integral methods)

As an alternative to modeling the Reynolds stresses one can model mean flow profile directly. For simple 2-D flows this approach is quite food and will be used in this course. For complex and 3-D flows generally not successful. Consider the shape of turbulent velocity profiles.

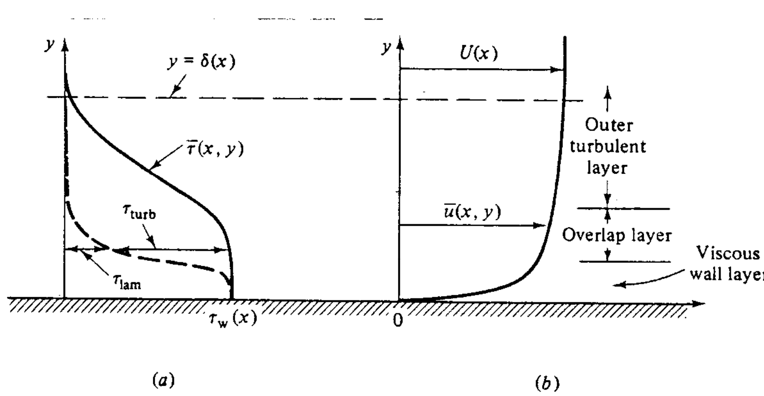

Fig. 6.8 Typical velocity and shear distributions in turbulent flow near a wall: (a) shear; (b) velocity. (measurements)

Note that very near the wall $\tau_{laminar}$ must dominate since $-\rho\overline{u_i u_j} = 0$ at the wall (y = 0) and in the outer part turbulent stress will dominate. This leads to the three layer concept:

Inner layer: viscous stress dominates

Outer layer: turbulent stress dominates

Overlap layer: both types of stress important

1. <u>laminar sub-layer</u> (viscous shear dominates)

$u = f(\mu, \tau_w, \rho, y)$ note: not $f(\delta)$

From dimensional analysis $u^+ = f(y^+)$ law-of-the-wall

$$u^+ = y^+$$

where: $$u^+ = \frac{u}{u^*}$$

$$u^* = \text{friction velocity} = \sqrt{\tau_w / \rho}$$

$$y^+ = \frac{yu^*}{\nu}$$

very near the wall:

$$\tau \sim \tau_w \sim \text{constant} = \mu \frac{du}{dy} \quad \Rightarrow \quad u = cy \quad \text{or} \quad u^+ = y^+$$

i.e.,

$$u^+ = y^+ \qquad 0 < y^+ < 5 \qquad y^+ = \frac{yu^*}{\gamma} \qquad y = r_o - r$$

$$u^* = \sqrt{\frac{\tau_o}{\rho}}$$

2. outer layer (turbulent shear dominates)

$$(U_e - u)_{outer} = g(\delta, \tau_w, \rho, y)$$

note: independent of μ and actually also depends on $\frac{dp}{dx}$

From dimensional analysis

$$\frac{U_e - u}{u^*} = f\left(\frac{y}{\delta}\right) \qquad \text{velocity defect law}$$

3. <u>overlap layer</u> (viscous and turbulent shear important)

In order for the inner and outer layers to merge smooth

$$u^+ = \frac{1}{\kappa} \ln y^+ + B \qquad 20 < y^+ < 10^5 \qquad \text{log-law}$$

$$\kappa = .41 \qquad B = 5.5$$

FIGURE 10.4
Apparent shear stress in a pipe. [After Laufer (23)]

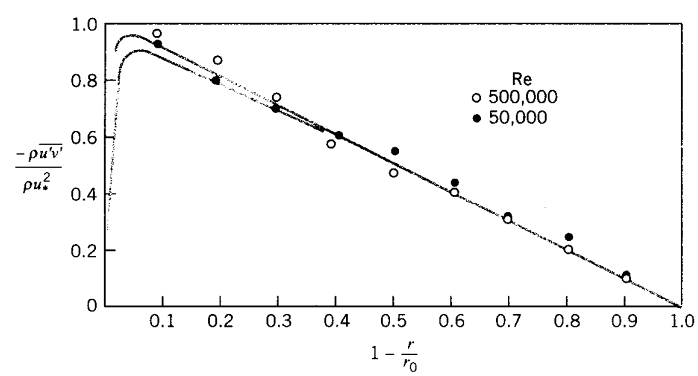

FIGURE 10.5
Velocity distribution for smooth pipes. [After Schlichting (36)]

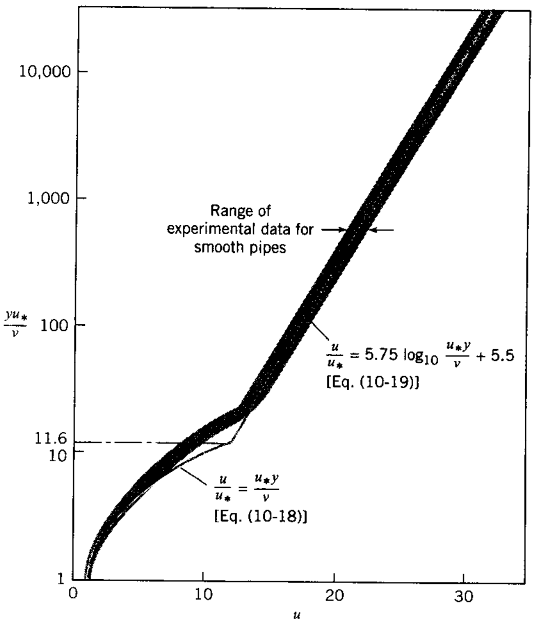

FIGURE 9.9
Velocity distribution in a turbulent boundary layer.

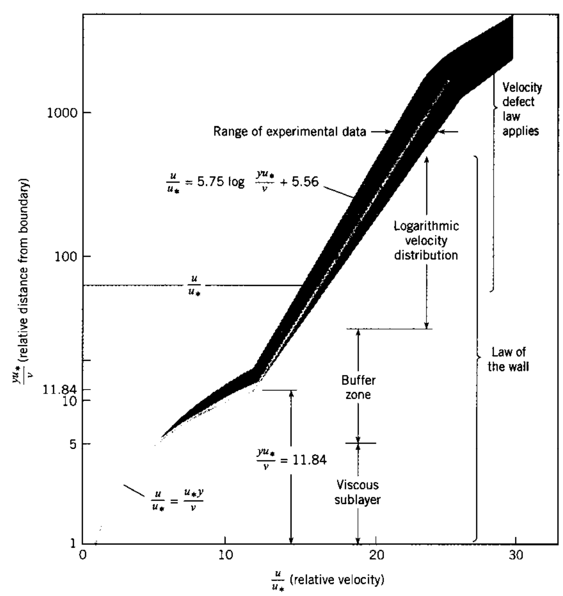

FIGURE 9.11

Velocity distribution in a turbulent boundary layer–linear scales.

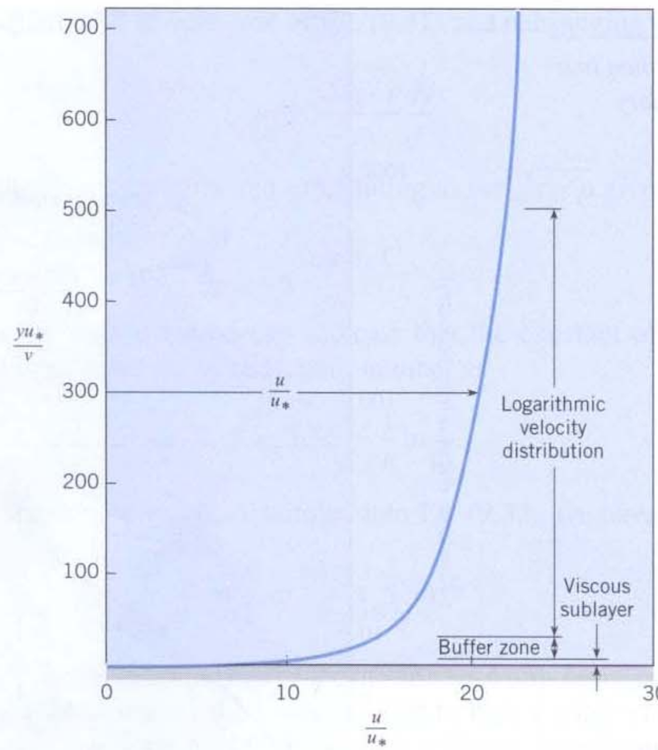

FIGURE 9.12

Velocity-defect law for boundary layers. [After Rouse (10)].

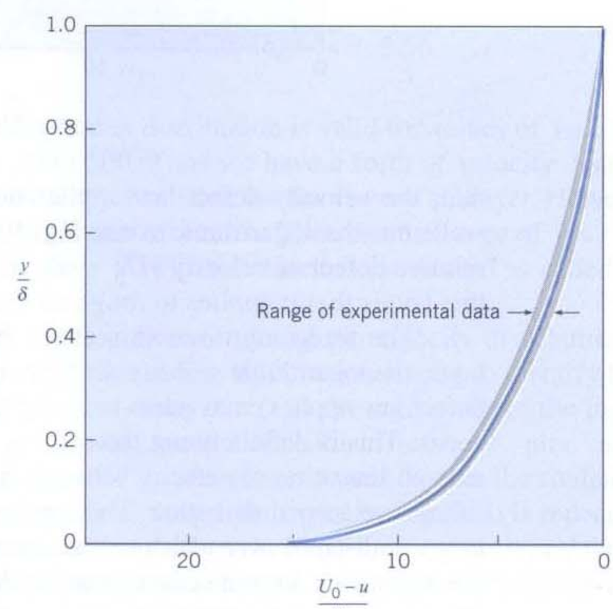

Note that the y^+ scale is logarithmic and thus the inner law only extends over a very small portion of δ

Inner law region < .2δ

And the log law encompasses most of the boundary-layer. Thus as an approximation one can simply assume

$$\frac{u}{u^*} = \frac{1}{\kappa} \ln y + B \qquad u^+ = \sqrt{\tau_w / \rho} \qquad y^+ = \frac{yu^*}{\nu}$$

is valid all across the shear layer. This is the approach used in this course for turbulent flow analysis. The approach is a good approximation for simple and 2-D flows (pipe and flat plate), but does not work for complex and 3-D flows.

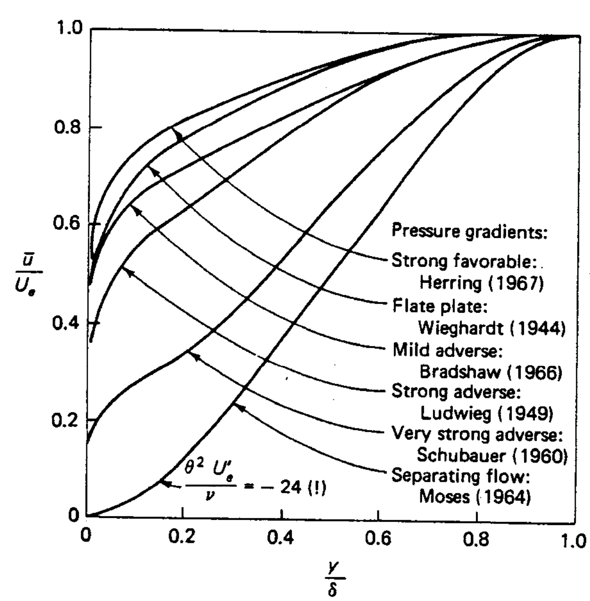

FIGURE 6-4
Experimental turbulent-boundary-layer velocity profiles for various pressure gradients.

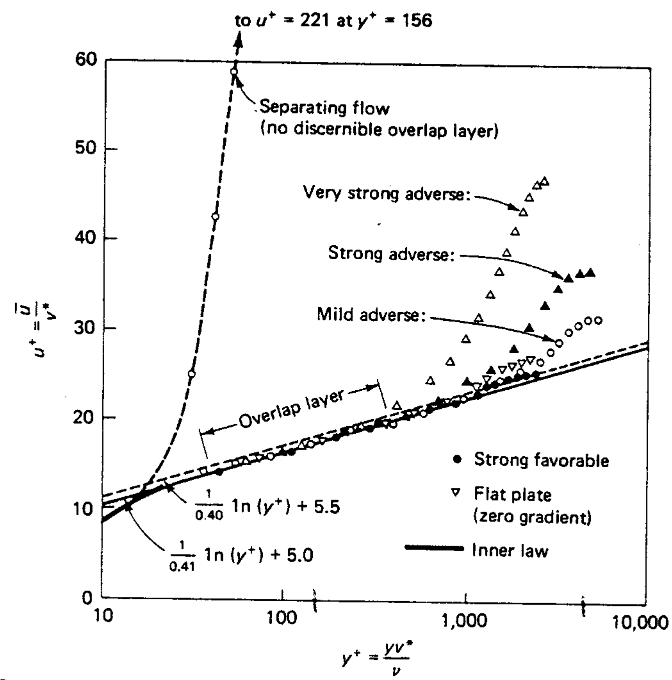

FIGURE 6-5
Replot of the velocity profiles of Fig. 6-4 using inner-law variables y^+ and u^+.

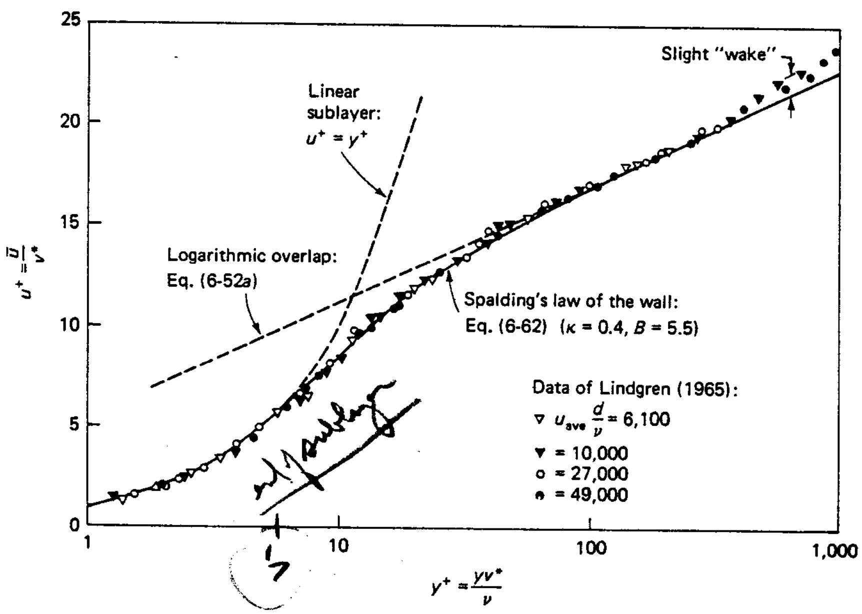

FIGURE 6-6
Comparison of Spalding's inner-law expression with the pipe-flow data of Lindgren (1965).

Velocity Distribution and Resistance in Smooth Pipes

Assume log-law is valid across entire pipe

$$u^+ = \sqrt{\frac{\tau_w}{\rho}} =$$ friction velocity

$$\frac{u(r)}{u^*} = \frac{1}{\kappa}\ln\frac{(r_o - r)u^*}{\nu} + B$$

$$\kappa = .41$$

$$B = 5.5$$

$$\overline{V} = \frac{Q}{A} = \frac{\int_0^{r_o} u(r) 2\pi r dr}{\pi r_o^2} = \frac{1}{2}u^*\left\{\frac{2}{\kappa}\ln\frac{r_o u^*}{\nu} + 2B - \frac{3}{\kappa}\right\}$$

drop over bar: $$\frac{V}{u^*} = 2.44\ln\underbrace{\frac{r_o u^*}{\nu}}_{\frac{1}{2}\mathrm{Re}\left(\frac{f}{8}\right)^{1/2}} + 1.34 = \left(\frac{\rho V^2}{\tau_o}\right)^{1/2} = \left(\frac{8}{f}\right)^{1/2}$$

$$\frac{1}{\sqrt{f}} = 1.99\log\left(\mathrm{Re}\, f^{1/2}\right) - 1.02$$

constants adjusted using data $$\Rightarrow \frac{1}{\sqrt{f}} = 2\log\left(\mathrm{Re}\, f^{1/2}\right) - .8 \qquad \mathrm{Re} > 3000$$

Power law $$\Rightarrow f \sim .316\mathrm{Re}^{-1/4} \qquad 4000 < \mathrm{Re} < 10^5$$

$$h_f = -\Delta h = -\left(\frac{\Delta p}{\gamma} + \Delta z\right) = f\frac{L}{D}\frac{V^2}{2g}$$

$$h_f = .316\left(\frac{\mu}{\rho VD}\right)^{1/4}\frac{L}{D}\frac{V^2}{2g}$$

$$h_f \propto V^{1.75}$$

(recall $h_f \propto V$ for laminar flow)

Other useful relationships

Power law fit to velocity profile:

$$\frac{u}{u_{\max}} = \left(1 - \frac{r}{r_o}\right)^m$$

$$m = m(\mathrm{Re})$$

$$\frac{u_{\max}}{u^*} = \frac{1}{\kappa}\ln\frac{r_o u^*}{r} + B$$

$$\frac{V}{u_{\max}} = \left(1 + 1.33 f^{1/2}\right)^{-1}$$

TABLE 10.1 EXPONENTS FOR POWER-LAW EQUATION AND RATIO OF MEAN TO MAXIMUM VELOCITY

Re →	4×10^3	2.3×10^4	1.1×10^5	1.1×10^6	3.2×10^6
m →	$\frac{1}{6.0}$	$\frac{1}{6.6}$	$\frac{1}{7.0}$	$\frac{1}{8.8}$	$\frac{1}{10.0}$
$\overline{V}/V_{\max}$ →	0.791	0.807	0.817	0.850	0.865

SOURCE: Schlichting (36). Used with permission of the McGraw-Hill Companies.

Viscous Distribution and Resistance – Rough Pipes

For laminar flow, effect of roughness is small; however, for turbulent flow the effect is large. Both laminar sublayer and overlap layer are affected.

Inner layer:

$$u = u(y, k, \rho, \tau_w)$$

$$u^+ = u^+(y/k)$$

not function of μ as was case for smooth pipe (or wall)

Outer layer: unaffected

Overlap layer:

$$u_R^+ = \frac{1}{\kappa}\ln\frac{y}{k} + \text{constant} \qquad \text{rough}$$

$$u_S^+ = \frac{1}{\kappa}\ln y^+ + B \qquad \text{smooth}$$

$$u_S^+ - u_R^+ = \underbrace{\frac{1}{\kappa}\ln k^+ + \text{constant}}_{\Delta B(k^+)} \qquad k^+ = \frac{ku^*}{\nu}$$

i.e., rough-wall velocity profile shifts downward by $\Delta B(k^+)$, which increases with k^+.

three regions of flow depending on k^+

1. $k^+ < 5$ hydraulically smooth (no effect of roughness)
2. $5 < k^+ < 70$ transitional roughness (Re dependence)
3. $k^+ > 70$ fully rough (independent Re)

For 3, $\Delta B = \frac{1}{\kappa}\ln k^+ - 3.5$ from data

$$u^+ = \frac{1}{\kappa}\ln\frac{y}{k} + 8.5 \neq f(\mathrm{Re})$$

$$\frac{V}{u^*} = 2.44\ln\frac{D}{k} + 3.2$$

$$\frac{1}{f^{1/2}} = -2\log\frac{k/D}{3.7}$$

fully rough flow

<u>Composite Log-Law</u>

$$u^+ = \underbrace{\frac{1}{\kappa}\ln y^+ + B}_{\text{Smooth wall log law}} - \Delta B(k^+)$$

$$u^+ = \frac{1}{\kappa}\ln y^+ + \underbrace{B - \Delta B(k^+)}_{B^*}$$

$B^* = 5 - \frac{1}{\kappa}\ln(1 + .3k^+)$ from data

$$\frac{1}{f^{1/2}} = -2\log\left[\frac{k/D}{3.7} + \frac{2.51}{\mathrm{Re}\, f^{1/2}}\right] \quad \text{Moody Diagram}$$

$$= 1.14 - 2\log\left(\frac{k_s}{D} + \frac{9.35}{\mathrm{Re}\, f^{1/2}}\right)$$

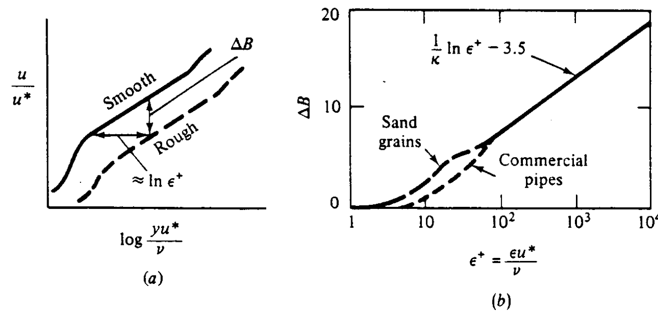

Fig. 6.12 Effect of wall roughness on turbulent pipe-flow velocity profiles: (*a*) logarithm-law downshift; (*b*) correlation with roughness

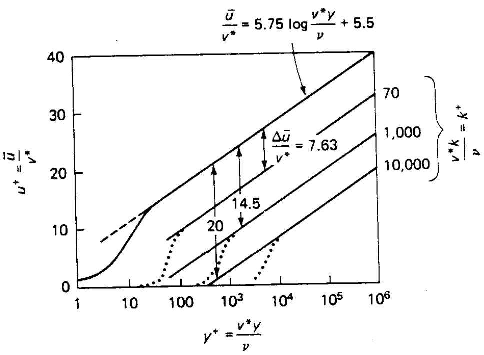

FIGURE 6-11
Experimental rough-pipe velocity profiles by Scholz (1955), showing the nward shift ΔB of the logarithmic overlap layer.

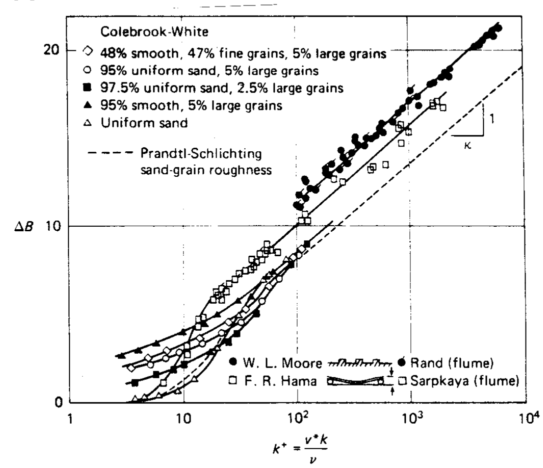

FIGURE 6-12
Composite plot of the profile-shift parameter $\Delta B(k^+)$ for various roughness geometries, as compiled by Clauser (1956).

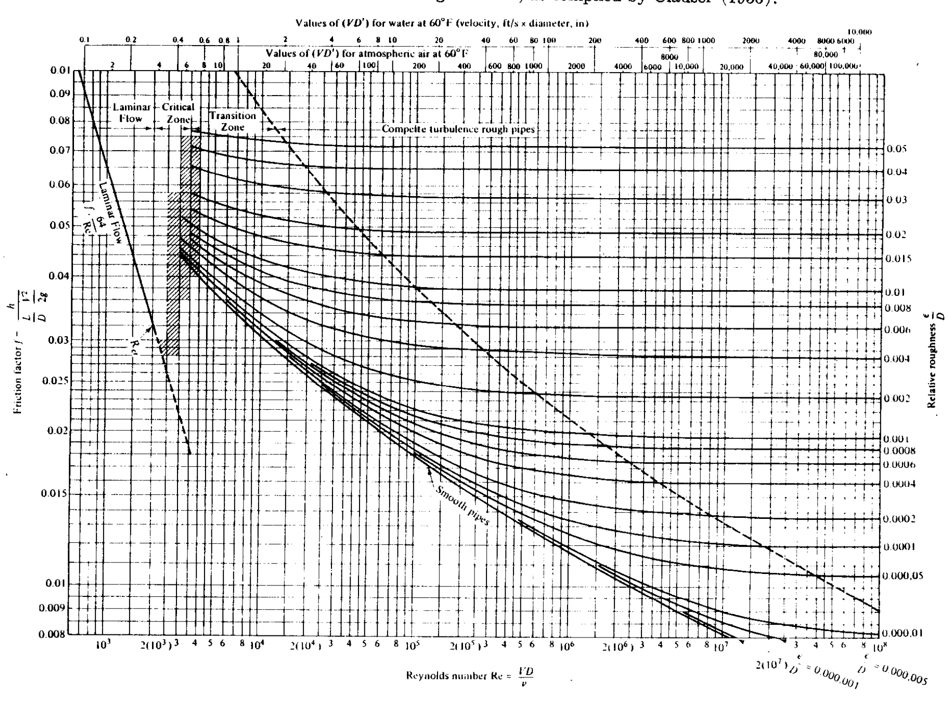

Fig. 6.13 The Moody chart for pipe friction with smooth and rough walls. (*From Ref. 8, by permission of the ASME.*)

FIGURE 10.7

Resistance coefficient f *versus Re for sand-roughened pipe. [After Nikuradse (30)]*

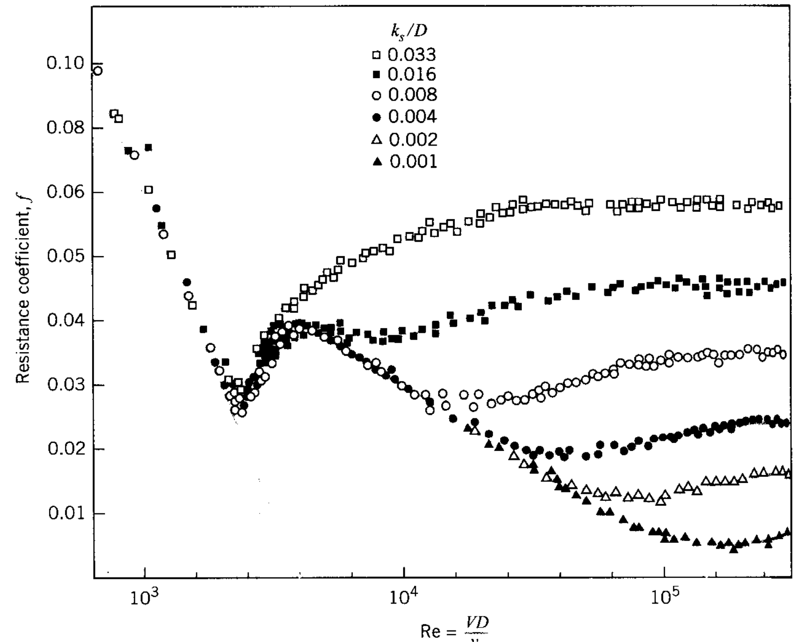

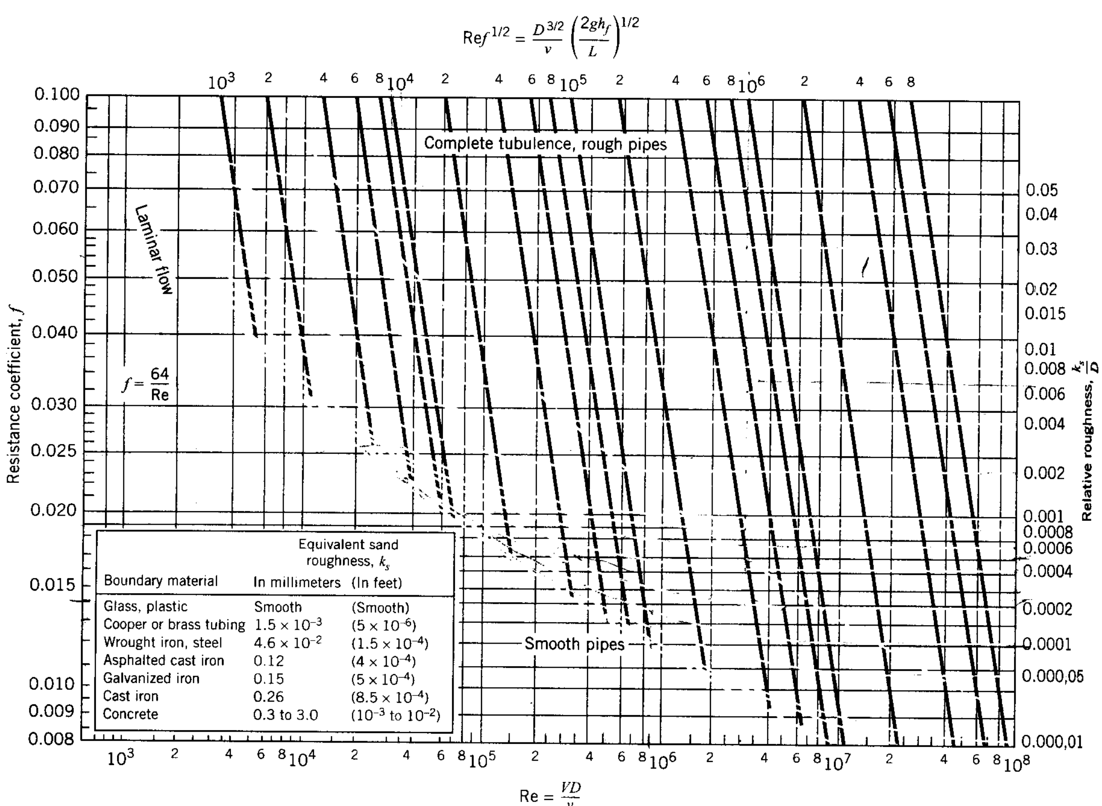

Boundary material	Equivalent sand roughness, k_s In millimeters	(In feet)
Glass, plastic	Smooth	(Smooth)
Cooper or brass tubing	1.5×10^{-3}	(5×10^{-6})
Wrought iron, steel	4.6×10^{-2}	(1.5×10^{-4})
Asphalted cast iron	0.12	(4×10^{-4})
Galvanized iron	0.15	(5×10^{-4})
Cast iron	0.26	(8.5×10^{-4})
Concrete	0.3 to 3.0	$(10^{-3}$ to $10^{-2})$

FIGURE 10.8

Resistance coefficient f *versus Re. Reprinted with minor variations. [After Moody (29). Reprinted with permission from the A.S.M.E.]*

FIGURE 10.9

Relative roughness for various kinds of pipe. [After Moody (29). Reprinted with permission from the A.S.M.E.]

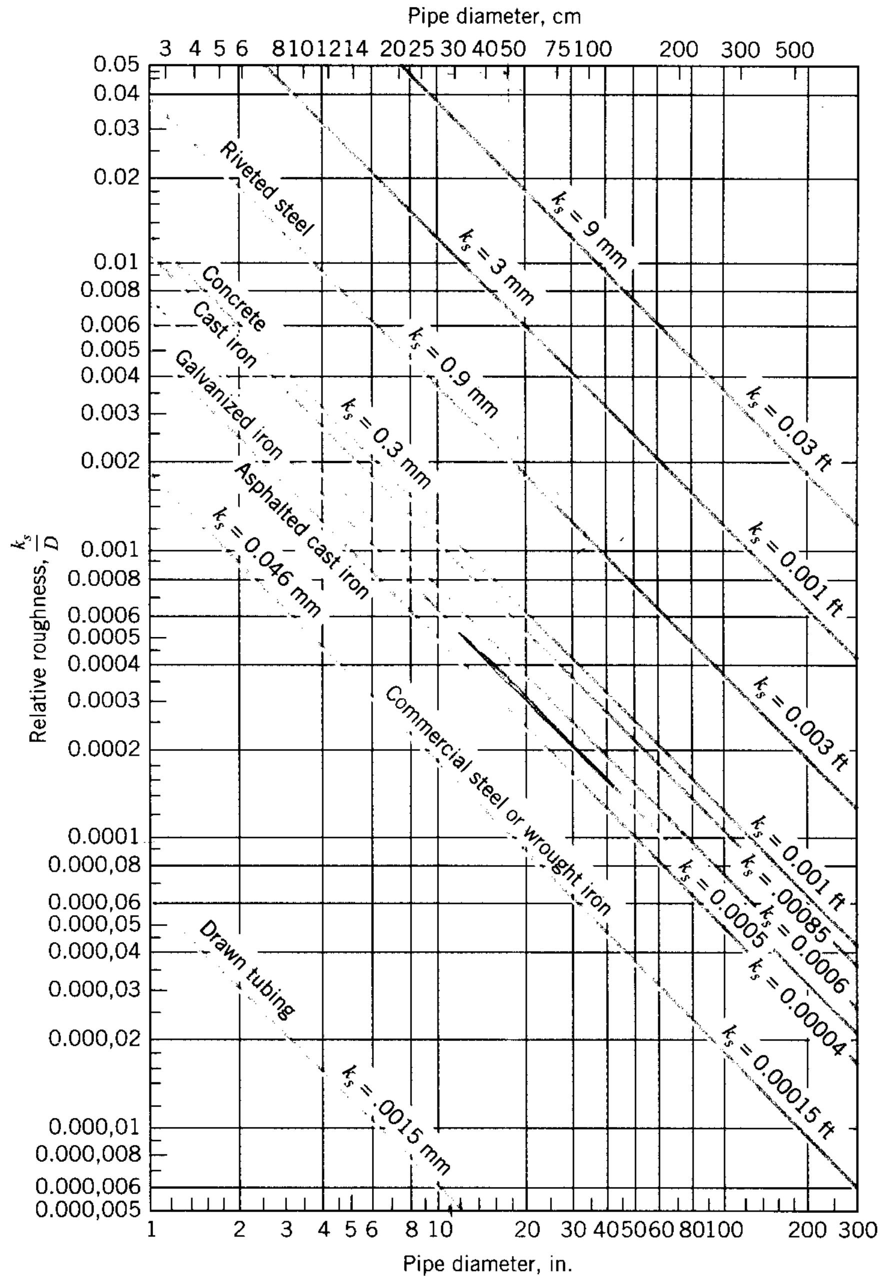

There are basically three types of problems involved with uniform flow in a single pipe:

1. Determine the head loss, given the kind and size of pipe along with the flow rate, Q = A*V
2. Determine the flow rate, given the head, kind, and size of pipe
3. Determine the pipe diameter, given the type of pipe, head, and flow rate

1. Determine the head loss
   The first problem of head loss is solved readily by obtaining f from the Moody diagram, using values of Re and k_s/D computed from the given data. The head loss h_f is then computed from the Darcy-Weisbach equation.

   $$f = f(Re_d, k_s/D)$$

   $$h_f = f\frac{L}{D}\frac{V^2}{2g} = -\Delta h \qquad \Delta h = \left(\frac{p_2}{\gamma} + z_2\right) - \left(\frac{p_1}{\gamma} + z_1\right)$$

   $$= -\Delta\left(\frac{p}{\gamma} + z\right)$$

   $$Re_d = Re_d(V, D)$$

2. Determine the flow rate
   The second problem of flow rate is solved by trial, using a successive approximation procedure. This is because both Re and f(Re) depend on the unknown velocity, V. The solution is as follows:

1) solve for V using an assumed value for f and the Darcy-Weisbach equation

$$V = \underbrace{\left[\frac{2gh_f}{L/D}\right]^{1/2}}_{\text{known from given data}} \cdot f^{-1/2}$$

note sign

2) using V compute Re
3) obtain a new value for f = f(Re, k_s/D) and reapeat as above until convergence

Or can use $\mathrm{Re}\, f^{1/2} = \dfrac{D^{3/2}}{\nu}\left(\dfrac{2gh_f}{L}\right)^{1/2}$

scale on Moody Diagram

1) compute $\mathrm{Re}\,f^{1/2}$ and k_s/D
2) read f
3) solve V from $h_f = f\dfrac{L}{D}\dfrac{V^2}{2g}$
4) Q = VA

3. Determine the size of the pipe
   The third problem of pipe size is solved by trial, using a successive approximation procedure. This is because h_f, f, and Q all depend on the unknown diameter D. The solution procedure is as follows:

1) solve for D using an assumed value for f and the Darcy-Weisbach equation along with the definition of Q

$$D = \underbrace{\left[\frac{8LQ^2}{\pi^2 g h_f}\right]^{1/5}}_{\text{known from given data}} \cdot f^{1/5}$$

2) using D compute Re and k_s/D

3) obtain a new value of $f = f(Re, k_s/D)$ and reapeat as above until convergence

<u>Flows at Pipe Inlets and Losses From Fittings</u>

For real pipe systems in addition to friction head loss these are additional so called minor losses due to

1. entrance and exit effects
2. expansions and contractions
3. bends, elbows, tees, and other fittings
4. valves (open or partially closed)

can be large effect

For such complex geometries we must rely on experimental data to obtain a loss coefficient

$$K = \frac{h_m}{\frac{V^2}{2g}}$$

head loss due to minor losses

In general,

$$K = K(\text{geometry}, \underbrace{Re, \varepsilon/D}_{\text{dependence usually not known}})$$

Loss coefficient data is supplied by manufacturers and also listed in handbooks. The data are for turbulent flow conditions but seldom given in terms of Re.

Modified Energy Equation to Include Minor Losses:

$$\frac{p_1}{\gamma} + z_1 + \frac{1}{2g}\alpha_1 V_1^2 + h_p = \frac{p_2}{\gamma} + z_2 + \frac{1}{2g}\alpha_2 V_2^2 + h_t + h_f + \sum h_m$$

$$h_m = K\frac{V^2}{2g}$$

Note: Σh_m does not include pipe friction and e.g. in elbows and tees, this must be added to h_f.

1. Flow in a bend:

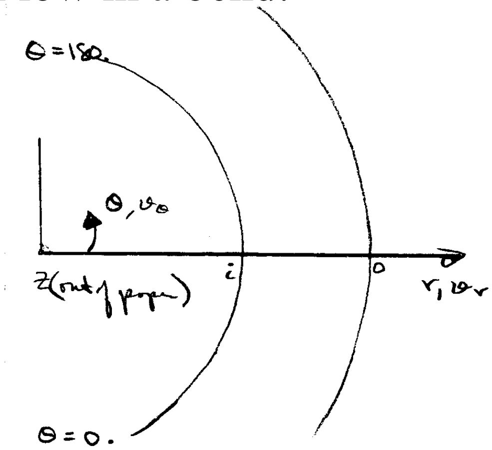

$$\underbrace{-\frac{1}{r}v_\theta^2}=-\frac{1}{\rho}\frac{\partial p}{\partial r}$$

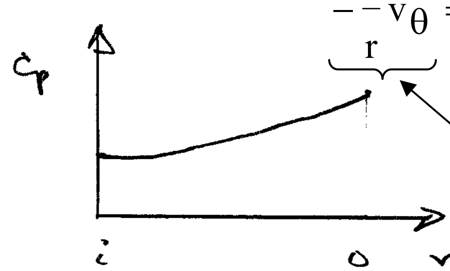

i.e. $\dfrac{\partial p}{\partial r}>0$ which is an adverse pressure gradient in r direction. The slower moving fluid near wall responds first and a swirling flow pattern results.

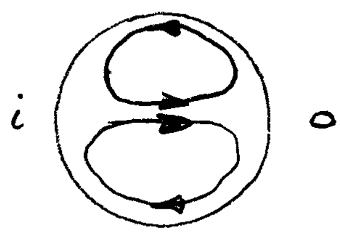

This swirling flow represents an energy loss which must be added to the h_L.

Also, flow separation can result due to adverse longitudinal pressure gradients which will result in additional losses.

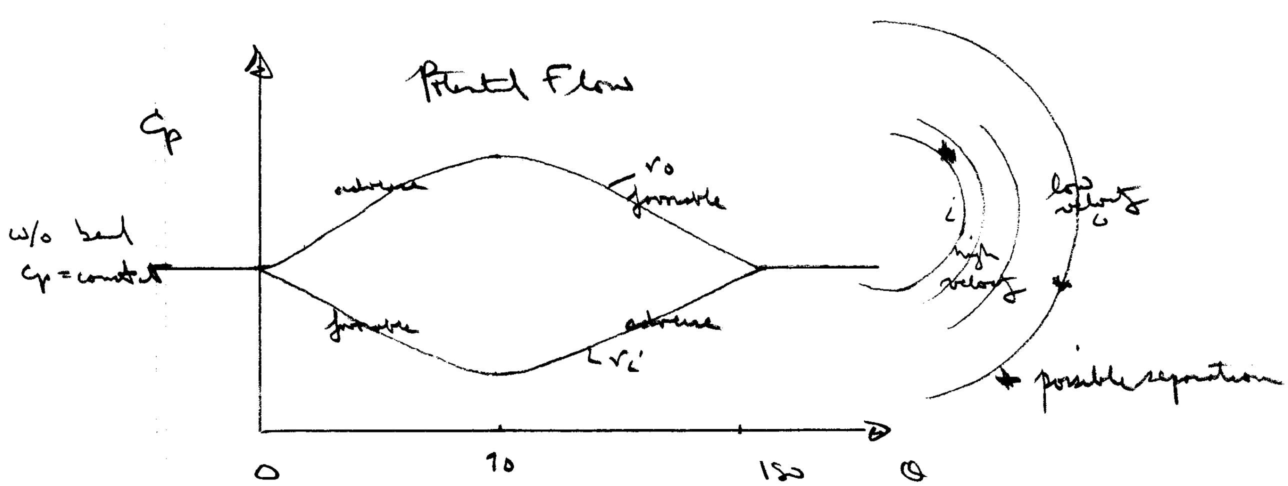

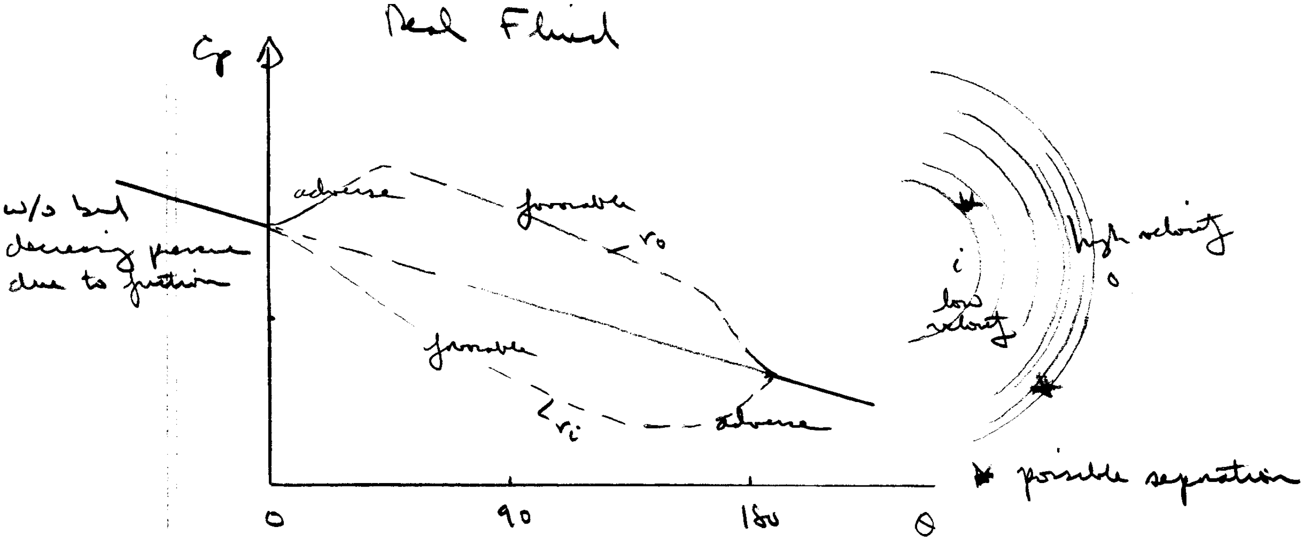

This shows potential flow is not a good approximate in internal flows (except possibly near entrance)

2. Valves: enormous losses

3. Entrances: depends on rounding of entrance

4. Exit (to a large reservoir): K = 1
i.e., all velocity head is lost

5. Contractions and Expansions
$\underbrace{\text{sudden}}$ or gradual

theory for expansion:

$$h_L = \frac{(V_1 - V_2)^2}{2g}$$

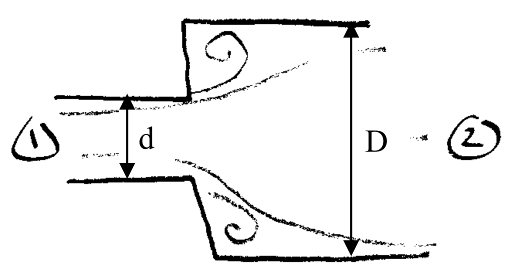

from continuity, momentum, and energy
(assuming $p = p_1$ in separation pockets)

$$\Rightarrow \quad K_{SE} = \left(1 - \frac{d^2}{D^2}\right)^2 = \frac{h_m}{V_1^2 / 2g}$$

no theory for contraction:

$$K_{SC} = .42\left(1 - \frac{d^2}{D^2}\right)$$

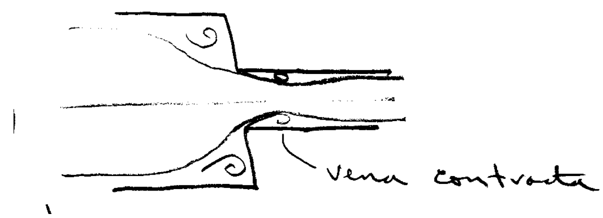

from experiment

If the contraction or expansion is gradual the losses are quite different. A gradual expansion is called a diffuser. Diffusers are designed with the intent of raising the static pressure.

$$C_p = \frac{p_2 - p_1}{\frac{1}{2}\rho V_1^2}$$

$$C_{p_{ideal}} = 1 - \left(\frac{A_1}{A_2}\right)^2$$ Bernoulli and continuity equation

$$K = \frac{h_m}{V^2 / 2g} = C_{p_{ideal}} - C_p$$ Energy equation

Actually very complex flow and

$$C_p = C_p(\text{geometry}, \underbrace{\text{inlet flow conditions}})$$

i.e., fully developed (long pipe) reduces C_p
thin boundary layer (short pipe) high C_p
(more uniform inlet profile)

FIGURE 10.10
Flow characteristics at a pipe inlet (not to scale).

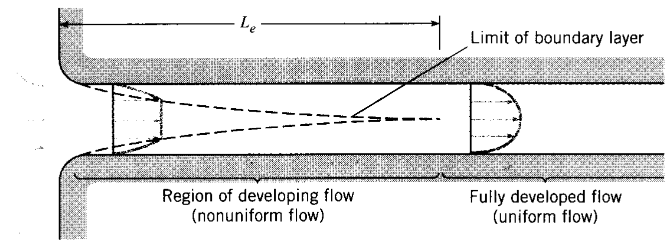

FIGURE 10.11
Distribution of velocity and pressure in the inlet region of a pipe [Barbin and Jones (3)].
(a) Velocity distribution.
(b) Pressure distribution.

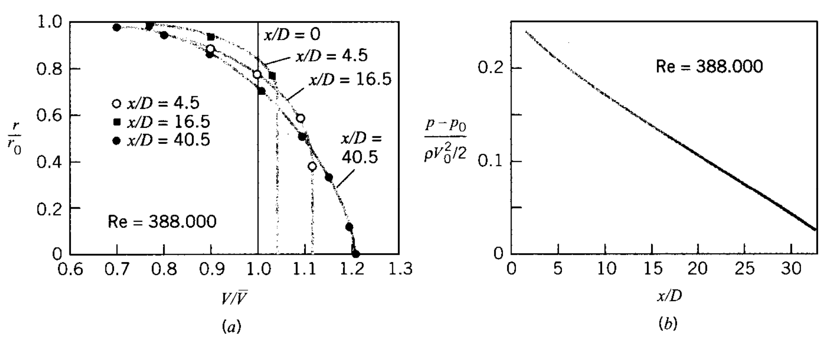

Turbulent flow

FIGURE 10.12
Flow at a sharp-edged inlet.

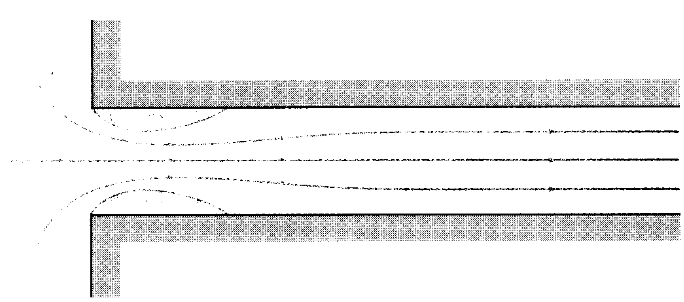

K = .5

FIGURE 10.13
Flow pattern in an elbow.

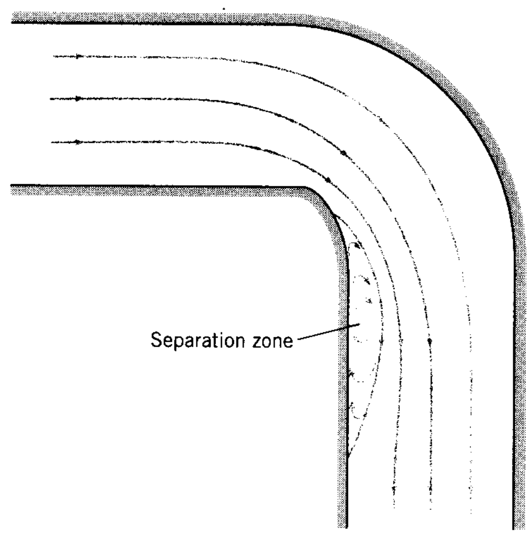

See textbook Table 8.2 for a table of the loss coefficients for pipe components

TABLE 10.2 LOSS COEFFICIENTS FOR VARIOUS TRANSITIONS AND FITTINGS

Description	Sketch	Additional Data		K	Source
Pipe entrance	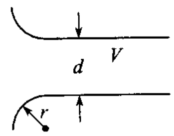	r/d		K_e	(2)*
		0.0		0.50	
		0.1		0.12	
$h_L = K_e V^2/2g$		>0.2		0.03	
Contraction	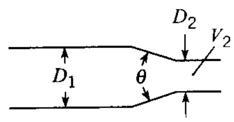		K_C	K_C	
		D_2/D_1	$\theta = 60°$	$\theta = 180°$	(2)
		0.0	0.08	0.50	
		0.20	0.08	0.49	
		0.40	0.07	0.42	
		0.60	0.06	0.27	
		0.80	0.06	0.20	
$h_L = K_C V_2^2/2g$		0.90	0.06	0.10	
Expansion	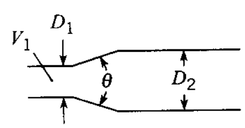		K_E	K_E	
		D_1/D_2	$\theta = 20°$	$\theta = 180°$	(2)
		0.0		1.00	
		0.20	0.30	0.87	
		0.40	0.25	0.70	
		0.60	0.15	0.41	
$h_L = K_E V_1^2/2g$		0.80	0.10	0.15	
90° miter bend	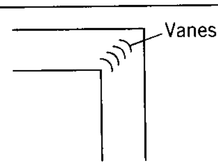	Without vanes		$K_b = 1.1$	(37)
		With vanes		$K_b = 0.2$	(37)
90° smooth bend	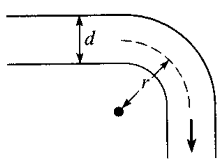	r/d			(5) and (19)
		1		$K_b = 0.35$	
		2		0.19	
		4		0.16	
		6		0.21	
		8		0.28	
		10		0.32	
Threaded pipe fittings	Globe valve—wide open	$K_v = 10.0$			(37)
	Angle valve—wide open	$K_v = 5.0$			
	Gate valve—wide open	$K_v = 0.2$			
	Gate valve—half open	$K_v = 5.6$			
	Return bend	$K_b = 2.2$			
	Tee				
	straight-through flow	$K_t = 0.4$			
	side-outlet flow	$K_t = 1.8$			
	90° elbow	$K_b = 0.9$			
	45° elbow	$K_b = 0.4$			

*Reprinted by permission of the American Society of Heating, Refrigerating and Air Conditioni
Engineers, Atlanta, Georgia, from the 1981 ASHRAE Handbook-Fundamentals.

FIGURE 10.14

EGL and HGL at a sharp-edged pipe entrance.

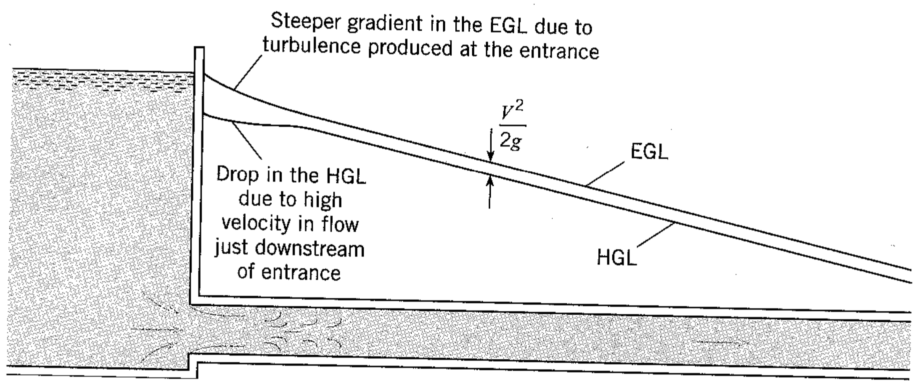

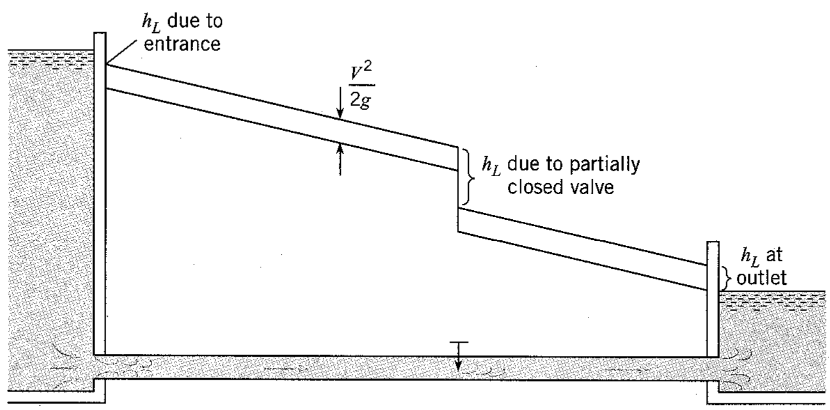

IGURE 10.15

ead losses in a pipe.